

An atmospheric pressure coaxial DBD reactor under bi-polar pulsed HV excitation

E Panousis¹, F Clément¹, K Proimadis², J-F Loiseau¹, B Held¹, L Marlin³

¹ *Laboratoire d' Electronique des Gaz et des Plasmas, Université de Pau et des Pays de l' Adour, Pau 64013, France*

² *Electrotechnic Materials Laboratory, University of Patras, Rion/Patras 26500, Greece*

³ *Atelier de Physique, Université de Pau et des Pays de l' Adour, Pau 64013, France*

An atmospheric pressure molecular Nitrogen Dielectric Barrier Discharge (DBD) under pulsed High Voltage excitation, is here shown. The DBD reactor used is of coaxial geometry with the dielectric covering only the active (High Voltage) electrode. The reactor has been conceived for surface treatment applications in spatial afterglow conditions, assured by the reactor's open geometry and the high gas flow. Primary experimental results are given in the framework of optical observations as well as current and voltage oscillogrammes when varying the HV signal's characteristics. A multi-filamentary regime characterizes the discharge, with filaments appearing to spread more homogeneously inside the discharge gap as the high voltage frequency increases.

1. Introduction

Dielectric Barrier Discharges (DBD's), originally proposed by Siemens in the 1800's [1], are still a subject of active research presenting numerous applications ranging from plasma display panels and biological decontamination to flow control and surface treatment [2-6]. DBD reactors are usually implemented by the deposition of an insulator over one or both metallic electrodes, the most frequently used dielectric materials being Pyrex, quartz, polymers and ceramics. The main advantage of DBD technology is the fact that it facilitates cold plasma generation in atmospheric pressure conditions. It is well known that under such conditions, electrical discharges between metallic electrodes are prone to arcing [7, 8]. The dielectric acts as a discharge current limiter, inhibiting thus the arc transition. With respect to experimental parameters, i.e. gas used, electrode geometry, HV waveform, amplitude and frequency, dielectric material used DBD plasmas present a homogeneous/diffuse or a filamentary character [9, 10], referring to the spatial localization and uniformity of the plasma channel over the inter-electrode interval in the direction normal to the discharge axis.

DBD cold plasmas exhibit an interesting chemistry: active species are formed during the discharge mainly via direct electron collisions with neutrals. These active species, the term here principally referring to electronically excited long-lived molecular states, due to their elevated potential energy can intervene in surface treatment applications [11, 12]. When working at atmospheric pressure, in the particular case of surface treatment, the elimination of costly vacuum systems that are needed for low pressure plasmas renders

atmospheric pressure DBD technology an attractive and cost-effective solution for both batch processing and single-piece applications.

The purpose of this work is to report primary experimental observations on a DBD set-up conceived for surface treatment applications at atmospheric pressure. The set-up's particularities are on one hand the use of an "open" DBD reactor, which allows the formation of a spatial afterglow induced by elevated gas flow and on the other hand a custom made bi-polar pulsed HV generator of varying frequency, rise-time and duty cycle, used to electrically supply the reactor.

In *part 2* experimental details will be given, presenting the reactor's design details, the HV generator and finally the complete set-up. Then, in *part 3*, experimental results will be reported in the framework of electrical measurements as well as optical observations.

2. Experimental details

This part is devoted to the presentation of the experimental arrangement. To begin with, the DBD reactor is presented, followed by an analysis of the HV generator. Finally, the complete experimental set-up is detailed.

2.1 DBD reactor

Figure 1 sketches a section of the DBD reactor, designed at the LEGP with the valuable assistance of the physics workshop of Pau University. It is shown that the reactor is of cylindrical coaxial geometry with axial gas flow. The H.V. signal is applied on the inner electrode, while the outer electrode is grounded. The dielectric coating used on the inner

electrode is Al_2O_3 and has a relative dielectric constant of $\epsilon_r = 4.5$.

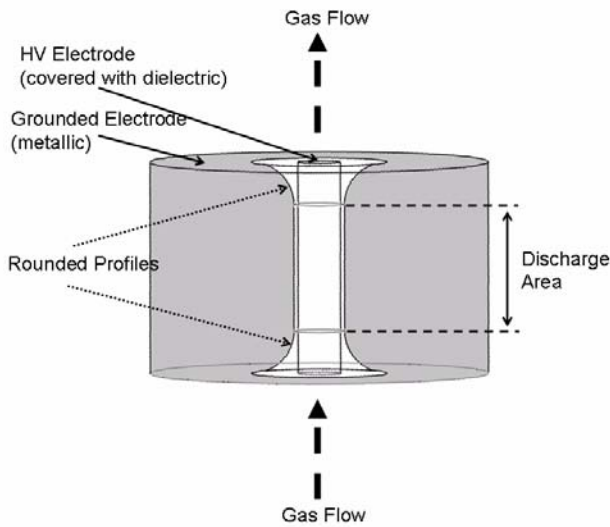


Figure 1: Sketch of the DBD reactor

As it can be observed, rounded (Rogowski) profiles have been employed on both extremities of the grounded metallic electrode in order to avoid local electric field enhancements due to point effects. Such geometrical inhomogeneities could favor a local discharge ignition and even produce arcing effects between, for instance, the inner electrode's top or bottom bases (where no coating was installed) and the grounded electrode. Thus, the actual discharge area is limited in a length smaller than the inner electrode's height, as figure 1 shows. It is noted that the discharge gap length equals $d=1\text{mm}$.

2.2 Bi-polar pulsed HV generator

A custom made bi-polar pulsed HV generator, fabricated on-demand by AcXys Technologies (Grenoble, France) has been used to electrically drive the DBD reactor.

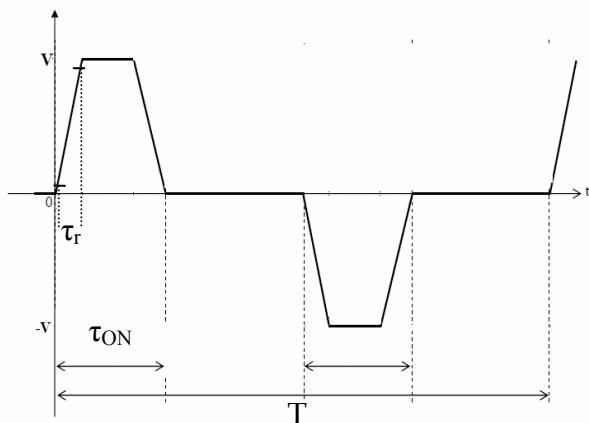


Figure 2: Idealized HV generator output signal

Figure 2 shows an idealized waveform of the HV generator's output signal. The generator, in the ideal case, delivers square high voltage pulses of alternating polarity. The HV generator's characteristics are as follows:

- The pulse rise time τ_r can be (only slightly) varied in the range from 0.2 to 0.6 kV/ns.
- The frequency ($f=1/T$) varies from 8 to 180 kHz
- Based on figure 2, one can define the HV signal's duty cycle as $r_c = 2 \times (\tau_{ON}/T)$, which varies from 0.05 to 0.4, provided that τ_{ON} is superior to 1 μsec .
- The voltage amplitude ranges from 0 to approximately 6 kV.

However, figure 2 presents only an idealized form of the generator's output. The actual HV signal, when no load (i.e. the DBD reactor) is connected at the generator is presented on figure 3. Here, only the positive voltage pulse is shown for $\tau_{ON}=5\mu\text{sec}$, since the negative one is symmetric.

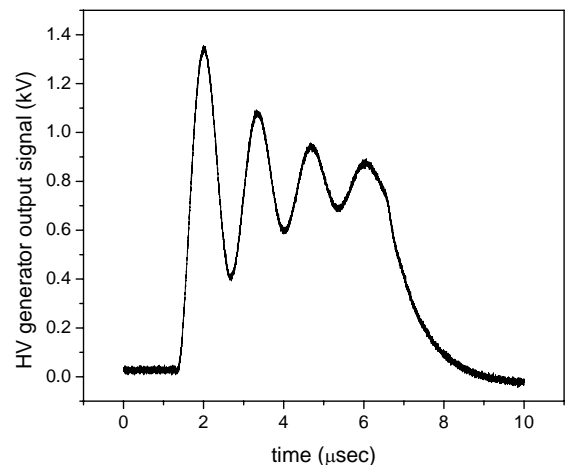


Figure 3: Positive voltage pulse at the generator's output (no load)

As it can be clearly seen on figure 3, the HV pulse exhibits important oscillations during the voltage ON phase that are superimposed to a DC component. This effect should be attributed to the HV generator's design principle: MOSFET controlled positive and negative square voltage pulses are applied to the primary of a HV transformer. The latter, being a non-ideal one, transforms the square pulses by adding the oscillations shown on figure 3. These oscillations, inherent to the use of the HV transformer, could be regarded as the result of a combination of RL circuit components representing the series part of the transformer's equivalent circuit [13].

2.3 Experimental Set-Up

Figure 4 (a) shows a schematic representation of the experimental set-up. The HV generator supplies electrically the DBD reactor via single-clone H.V. cables. The applied voltage is measured by a 1/1000 Tektronix P6015A voltage probe while the total current flowing in the circuit is measured by a Rogowski-type current probe. The electrical signals are visualized by means of a Tektronix 3054B oscilloscope (500MHz, 5 Gs/s) and then are digitized and transferred to a PC via Ethernet.

The gas used is nitrogen and the gas-flow controlled by a volume flow-meter, is provided by a cryogenic vessel. Gas flow values can be varied in the range of 1 to 100 SL/min.

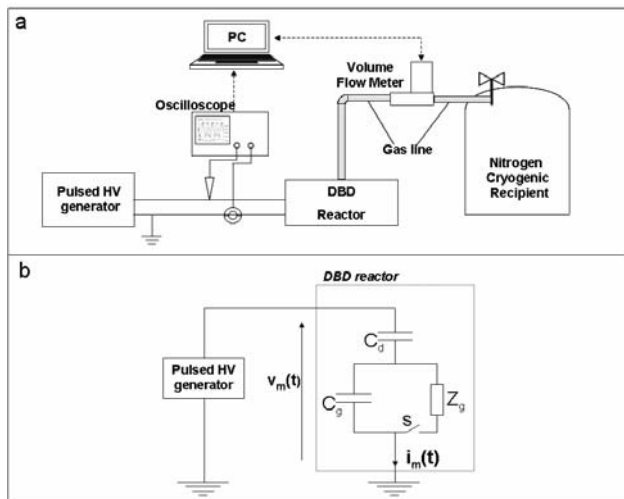


Figure 4: (a) Schematic representation of the experimental set-up (b) Electrical equivalent

Following a rather classical approach, the electrical equivalent of the above set-up is given in Figure 4(b). The DBD reactor is modeled by a capacitor C_d ($d \equiv$ dielectric) representing the solid dielectric, in series with the gas gap. The latter is the parallel combination of a C_g capacitor and a Z_g impedance ($g \equiv$ gas), corresponding respectively to the pure gas capacitance and the plasma impedance. The switch s , drawn on the electrical equivalent circuit, is fictional. It is used to denote that there is plasma activity only during a part of the period of the applied voltage. The measured applied voltage and total current flowing in the circuit are respectively denoted by $v_m(t)$ and $i_m(t)$. It is here noted that the current measured is the total discharge current, being the sum of a displacement and a conduction component.

3. Experimental observations - Discussion

Figure 5 shows a photograph of the discharge plasma ignited with the experimental set-up described above. The luminous blue-violet ring surrounding the active electrode can be distinguished, typical for a Nitrogen plasma, owing mainly to radiative de-excitations of the Second Positive System: $N_2(C^3\Pi_u) \rightarrow N_2(B^3\Pi_g) + h\nu$.



Figure 5: Discharge plasma snapshot

Under the conditions here investigated, the discharge presents visually a multi-filamentary character.

This fact is also verified by the measured current's waveform, which is shown on Figure 6 along with the applied voltage for both the positive and the negative HV pulse (the negative signals have been inverted for reasons of clarity). Here HV signal's frequency is equal to 20 kHz, $\tau_{ON}=2\mu\text{sec}$ and the gas flow is 25 SL/min. It can be observed that the discharge current, both in the positive and in the negative case is constituted by an aggregation of rapid peaks of quite high amplitude. Each peak denotes one or more probably a series of microdischarges that occur in different locations inside the gap, in an "instantaneous" way for the temporal resolution of the current set-up. These strong peaks also induce a rather marked monotonicity breaking on the voltage curves, as figure 6 shows. The fact that two peaks of higher amplitude seem to emerge in both cases, denotes an effect of local discharge ignition. In the case of a quasi-homogeneous spreading of discharge filaments inside the gap, one should expect that current peaks should present approximately the same amplitude. However, since one can distinguish particular peaks of clearly higher amplitude, it is thought that local inhomogeneities favour local discharge ignition. These effects could be either due

to centering problems of the inner electrode or to a non homogeneity on the thickness of the dielectric coating.

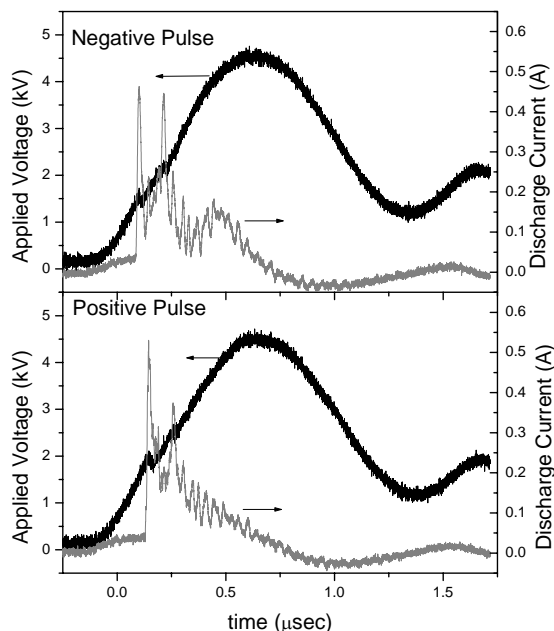


Figure 6: Measured voltage and current waveforms for the negative and positive HV pulse. (Negative signals have been inverted).

The hypothesis of local discharge ignition is strengthened by the low ignition voltage (below 2kV) denoting point effects, as well as by the fact that it is experimentally observed that when the voltage just reaches the onset threshold, the discharge ignites only in part of the circumference shown in figure 5. Then, a further increase of the applied voltage gives a visually uniform ignition in the way shown in figure 5.

A similar effect is exhibited when HV frequency is increased. It is visually observed that increasing frequency tends to give a more homogeneous visual aspect on the discharge, a fact which is also in accordance with electrical measurements. As figure 7 shows, the currents maxima tend to diminish with frequency to a plateau value, when the other electrical parameters are kept constant. In high (above 100 kHz) frequencies, all current peaks present the same amplitude, denoting a quasi-homogeneous spreading of the discharge filaments.

Following this primary analysis, thorough electrical and optical diagnostics of the current set-up are in progress and will be reported promptly.

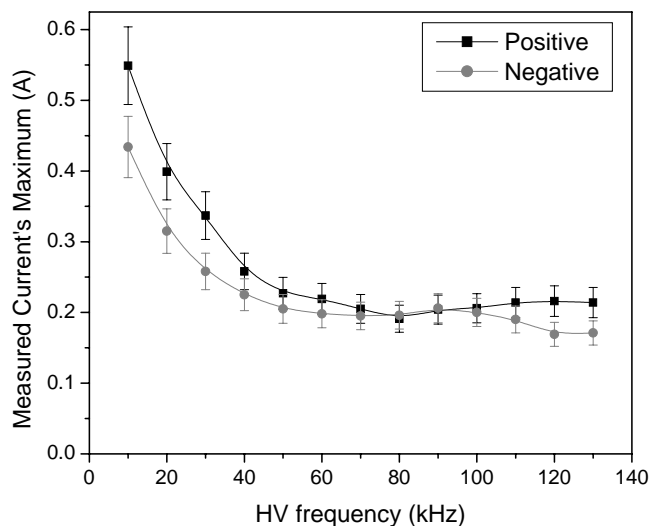


Figure 6: Absolute measured current's maxima for the negative and positive HV pulse.

Acknowledgments

This work is financially supported by a French national research program: ANR – PLASMAPAL

References

- [1] Kogelschatz U, *et al* Pure Appl. Chem., 71(10), 1819-1828, 1999
- [2] Reece Roth J, Physics of Plasmas 10(5), 2117-2126, 2003
- [3] Borgia G, *et al* Surface and Coatings Technology, 201 (6), 3074-3081, 2006
- [4] Kersten H, *et al* Surface and Coatings Technology, 86-87, 762-767, 1996
- [5] Boeuf J P, J. Phys. D: Appl. Phys. 36, R53-R79, 2003
- [6] Laroussi M., IEEE Trans. Plasma Sci., 30(4), 1409-1415, 2002
- [7] Massines F, *et al* Surface and Coatings Technology 174 –175, 8–14, 2003
- [8] Kogelschatz U and Salge J, "Chapter 13: High Pressure Plasmas: dielectric barrier and corona discharges-properties and technical applications" in "Low Temperature Plasma Physics" Wiley-VCH 2000
- [9] Kozlov K V, *et al* J. Phys. D: Appl. Phys. 38, 518–529, 2005
- [10] Kogelschatz U, IEEE Trans. Plasma Sci., 30(4), 1400-1408, 2002
- [11] Panousis E, *et al* Clément F, Loiseau J-F, Spyrou N, Held B, Thomachot M and Marlin L, Plasma Sources Sci. Technol. 15, 828–839, 2006
- [12] Panousis E, *et al* accepted for publication at "Surface and Coatings Technology" doi: 10.1016/j.surfcoat.2007.01.045
- [13] N Mohan, *et al* -1995- 'Power Electronics, Converters, Applications and Design' - J. Wiley